Oxygen and hydrogen sorption in thermally activated yttrium-based getter thin films for MEMS vacuum packaging

Charlotte Kutyla, Sylvain Lemettre, Clément Bessouet, Alain Bosseboeuf, Philippe Coste, Thierry Sauvage, Olivier Wendling, Aurelien Bellamy, Piyush Jagtap, Stephanie Escoubas, et al.

Oxygen and hydrogen sorption in thermally activated yttrium-based getter thin films for MEMS vacuum packaging

Charlotte Kutyla
C2N, Centre de Nanosciences et de Nanotechnologies, Université Paris-Saclay, CNRS, UMR 9001 91120 Palaiseau, France.
CEMHTI, Conditions Extrêmes et Matériaux : Haute Température et Irradiation, Université d'Orleans, UPR 3079 CNRS, 45071 Orléans Cedex 2, France.
charlotte.kutyla@c2n.upsaclay.fr

Alain Bosseboeuf
C2N, Centre de Nanosciences et de Nanotechnologies, Université Paris-Saclay, CNRS, UMR 9001 91120 Palaiseau, France.
alain.bosseboeuf@c2n.upsaclay.fr

Olivier Wendling
CEMHTI, Conditions Extrêmes et Matériaux : Haute Température et Irradiation, Université d'Orleans, UPR 3079 CNRS, 45071 Orléans Cedex 2, France.
olivier.wendling@cnrs-orleans.fr

Stéphanie Escoubas
IM2NP, Institut Matériaux Microélectronique Nanosciences de Provence, CNRS, UMR 7334, 13397 Marseille Cedex 20, France.
stephanie.escoubas@im2np.fr

Sylvain Lemettre
C2N, Centre de Nanosciences et de Nanotechnologies, Université Paris-Saclay, CNRS, UMR 9001 91120 Palaiseau, France.
sylvain.lemettre@c2n.upsaclay.fr

Philippe Coste
C2N, Centre de Nanosciences et de Nanotechnologies, Université Paris-Saclay, CNRS, UMR 9001 91120 Palaiseau, France.
philippe.coste@c2n.upsaclay.fr

Aurélien Bellamy
CEMHTI, Conditions Extrêmes et Matériaux : Haute Température et Irradiation, Université d'Orleans, UPR 3079 CNRS, 45071 Orléans Cedex 2, France.
aurelien.bellamy@cnrs-orleans.fr

Christophe Guichet
IM2NP, Institut Matériaux Microélectronique Nanosciences de Provence, CNRS, UMR 7334, 13397 Marseille Cedex 20, France.
christophe.guichet@im2np.fr

Johan Moulin
C2N, Centre de Nanosciences et de Nanotechnologies, Université Paris-Saclay, CNRS, UMR 9001 91120 Palaiseau, France.
johan.moulin@c2n.upsaclay.fr

Clément Bessouet
C2N, Centre de Nanosciences et de Nanotechnologies, Université Paris-Saclay, CNRS, UMR 9001 91120 Palaiseau, France.
clement.bessouet@c2n.upsaclay.fr

Thierry Sauvage
CEMHTI, Conditions Extrêmes et Matériaux : Haute Température et Irradiation, Université d'Orleans, UPR 3079 CNRS, 45071 Orléans Cedex 2, France.
thierry.sauvage@cnrs-orleans.fr

Piyush Jagtap
IM2NP, Institut Matériaux Microélectronique Nanosciences de Provence, CNRS, UMR 7334, 13397 Marseille Cedex 20, France.
piyush.jagtap@im2np.fr

Olivier Thomas
IM2NP, Institut Matériaux Microélectronique Nanosciences de Provence, CNRS, UMR 7334, 13397 Marseille Cedex 20, France.
olivier.thomas@im2np.fr

***Abstract*— Many microsensors need to operate in medium vacuum, which is obtained by low temperature vacuum packaging integrating a getter film. By a thermal activation during the sealing process, the getter film aims to compensate the outgassing of the inner surfaces of the micro-cavity and also leaks after sealing. Thin films of getter alloys were co-evaporated under ultra-high vacuum on silicon wafers. They were activated by annealing at temperatures ranging from 225 °C to 400 °C, during one hour under Argon atmosphere with traces of oxidizing species. Three complementary ion beam analysis techniques were performed to obtain depth profiles and to quantify the number of atoms of the different gaseous species absorbed by the getter films: Rutherford Backscattering Spectrometry (RBS), Nuclear Reaction Analysis (NRA) and Elastic Recoil Detection Analysis (ERDA). The results show that both oxygen and hydrogen diffuse inside the getter films. However, hydrogen tends to accumulate near the interface between film and substrate and starts to diffuse inside substrate as well. We demonstrated that the sorption of hydrogen by an yttrium-based getter film is tailored by its composition and depends on its degree of oxidation.**

Keywords*— *Yttrium alloys, oxidation, getter, thin films, low-temperature bonding

I. Introduction

Since the end of 20th century, getter materials were mainly studied and used in large vacuum facilities like particle accelerators, to provide Ultra and Extreme High Vacuum (UHV and XHV) [1]. Getter film has also an application in the vacuum packaging of microsensors. For several kinds of these devices a medium vacuum (10^{-4} mbar to 10^{-1} mbar) is required to get optimal performances during their whole lifetime (10 years or more) [2].

After unloading from the deposition set-up, a getter film is passivated by air exposure. Consequently, it must be thermally activated to re-generate a reactive metallic surface able to trap gases with a gas-and time-dependent rate. The activation results from the in-depth diffusion of the atoms of the passivating surface layer (mainly composed of oxides).

The role of a getter film for MEMS packaging is to compensate the outgassing during its sealing and also the residual leaks during its lifetime. The activation time and temperature of the getter must be limited to avoid device degradation. We consider in this work that the allowed thermal budget is at maximum one hour at a temperature of 350 °C.

Getter films previously investigated were mainly based on single element or alloys of transition metals of column IV (Ti, Zr, Hf) and V (V, Nb, Ta), respectively because of their high oxygen solubility or diffusivity [3]. Many of these films have already proved high performances for the sorption of oxygen. In this work, we investigate a new generation of getter materials for their application to MEMS vacuum packaging. We have chosen yttrium as a new base element because of its high affinity with oxygen, its large oxygen diffusivity as well as its high solubility limit (20 at. %) for hydrogen and its ability to easily form a highly stable YH_2 hydride [4] [5].

Here, we investigate the sorption capacity of oxygen and hydrogen for Y-based films when activated in an environment with relatively high partial pressures of oxidizing species, as found in MEMS packages.

II. Experimental Details

Thin films with thickness between 200 and 400 nm were deposited by UHV e-beam co-evaporation at room temperature on 100 mm in-diameter (100) silicon wafers. The background pressure before deposition was lower than 10^{-8} mbar. The pressure during evaporation did not exceed 10^{-7} mbar and was almost exclusively composed of H_2 gas (~90%) and of H_2O (~10%) as measured by mass spectrometry. The electron beam powers were adjusted to obtain a deposition rate of 0.5 nm/s for the main constituent of the getter film while deposition rates of the other constituents were chosen according to the desired composition.

To simulate the activation step occurring in a packaging process with a similar partial pressure of oxidizing species, the samples were annealed in a furnace under 99.9999 % pure Ar with traces of oxidizing gases, at 1 atm for 1 h and at temperatures ranging from 225 °C to 400°C. The argon flow during annealing was adjusted to 2000 sccm. This duration and range of temperature were chosen to correspond to the bonding temperatures commonly used in wafer-level packaging processes. For each annealing temperature, all samples of different compositions were annealed simultaneously.

The films sheet resistance was measured before and after annealing by the 4-point probe method at room temperature. The Temperature Coefficient of Resistance (TCR) was determined by using a method described previously [[9] Surface microstructure of as-deposited and annealed films was observed by Scanning Electron Microscopy (SEM). The in-plane mean grain size was estimated by using the mean linear intercept method following ASTM E112 standard. The microstructure and phase identification were carried out using an X-ray diffractometer (Philips-Panalytical) with Cu Kα source. The samples were analyzed in standard Bragg-Brentano geometry by varying the angle 2θ from 25° to 45°. The diffracted peaks were identified using reference data from powder samples.

Ion Beam Analysis (IBA) techniques were implemented to measure the stoichiometry of metal and light elements in getter films. The metallic elements composition and their in-depth homogeneity in films were controlled by Rutherford Backscattering Spectroscopy (RBS) with a 2 MeV 4He beam. The thin films characterization before and after annealing was completed by NRA (Nuclear Reaction Analysis) and ERDA (Elastic Recoil Detection Analysis) to determine oxygen and hydrogen atoms contents, respectively. The oxygen depth profile was measured by the $^{16}O(d, \alpha_0)^{14}N$ nuclear reaction with 900 keV deuterons. The α_0 particles are detected at 166° detection angle. ERDA was applied with a 2.8 MeV $^4He^+$ beam at 30° angle to determine the hydrogen depth profile through the nuclear reaction $^1H(^4He,^1H)^4He$.

The depth profiles were extracted from IBA spectra by using SIMNRA software [1999 Mayer] with SigmaCalc cross section [6] for NRA and ERDA. The O and H depth resolutions are close to 30-40 nm, depending on the film metallic composition.

III. Results and Discussion

A. Microstructure of as-deposited films

Y, Y-Al, Y-V, Y-V-Al, Y-Zr-Al, and Y-Ti with various compositions were deposited. The surface of all films,as observed by SEM, exhibits small grains in the 15-30 nm range. A columnar structure is observed in the cross-section of the pure yttrium film. It is highly crystallized and showed strong texture with an intense 002 Y peak observed by XRD. Y-Ti alloys have an hexagonal structure with a 002-peak shifting between the one of titanium and the one of yttrium, except for the $Y_{32}Ti_{68}$ which is in an amorphous state [7]. Y-Zr-Al alloys showed also an hcp crystalline structure with a 002-peak shifting between the one of yttrium (in Y rich alloy composition) and the one of zirconium, characteristic of a solid solution [8]. Y-V-Al alloys showed a broad and low intensity peak indicating a nanocrystalline structure, close to the amorphous state. Y-Al revealed a 002 Y-peak with a very low and spread intensity indicating a structure close to the amorphous state with small grains in the 10 nm range.

Electrical properties of as-deposited films are given in Fig. 1, with single metal data (Ti, Zr, V) extracted from [2019 Lemettre]. Alloyed films have a higher resistivity and lower TCR than single metal films. This is consistent with the fact that pure metals are less disordered than alloys, as shown by XRD analyses. The Mooij rule is followed since the alloys with a resistivity larger than 150 µΩ.cm present a negative TCR [11], at the noticeable exception of the single metal yttrium film. Despite its high resistivity of 172 µΩ.cm, its TCR is positive at 9 x 10^{-4} $°C^{-1}$. This exception may be due to the rather high hydrogen contamination of the film during its evaporation compared to Ti, Zr, and V. Such a contamination during evaporation was already observed by Huiberts et al [4]. A hydrogen over metal (H/M) atomic ratio of 0.28 was indeed measured in Y film by ERDA 14 days after deposition, while negligible amounts of H were measured in Ti, Zr, V single metal films. Hydrogen insertion in solid solution may greatly affect the resistivity of the Y film. This would also explain the large difference of resistivity between Yttrium thin film value and bulk Yttrium (59.6 µΩ.cm [10]). For Ti, Zr and V this difference is much lower. On the contrary, this incorporation of hydrogen in Y film might have less influence on the film TCR.

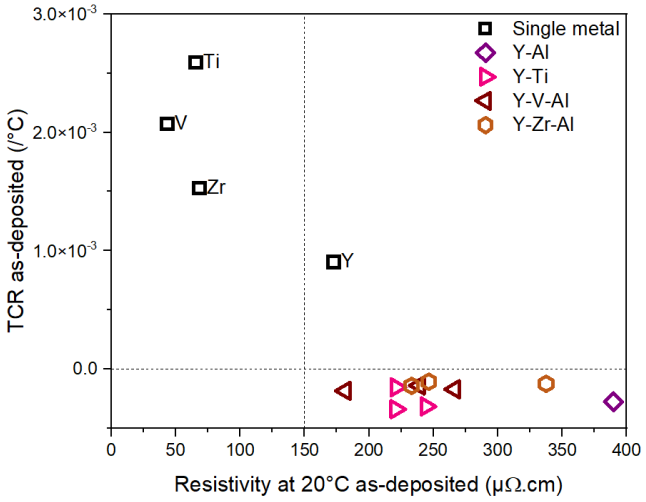

Fig. 1. TCR vs. resistivity of as-deposited films.

B. *Oxygen and hydrogen sorption in yttrium*

The oxygen and hydrogen depth profiles of yttrium film after different activation annealing are plotted in Fig.2. As mentioned above, a high H/M ratio is observed in the as-deposited Y film. An unexpected significant hydrogen content is also detected inside the silicon substrate. The oxygen profiles after annealing show a diffusion of oxygen from the surface to the bulk and also a thickening of the surface oxide. At temperature higher than 300 °C the oxygen distribution tends to be uniform. No oxygen diffusion in the substrate is observed. The hydrogen contents both inside the film and inside the substrate largely increase after thermal annealing up to 300 °C. This is attributed to the enhanced diffusion during annealing activation. However, after 350 °C annealing, the total hydrogen content in the film decreases. It might be related to yttrium oxidation which became high enough to inhibit the diffusion of incorporated hydrogen atoms [4].

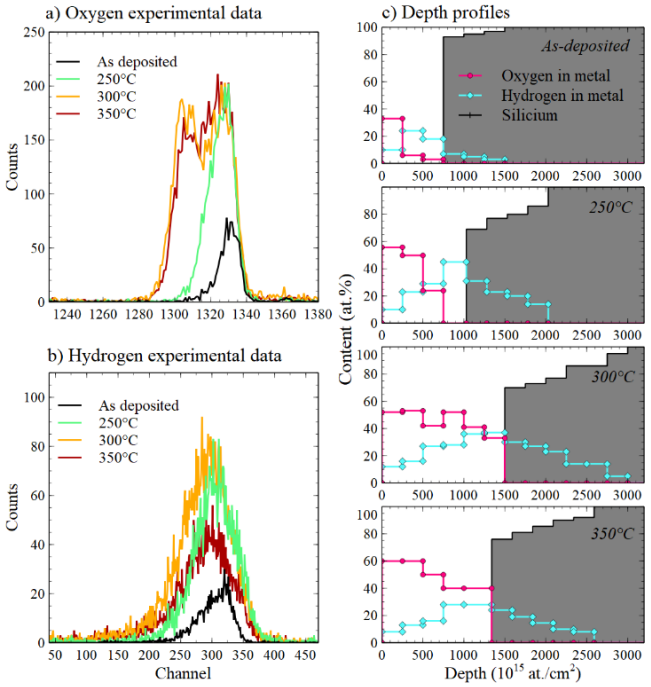

Fig. 2. a) Evolution of the oxygen and b) hydrogen peak obtained by NRA and ERDA as a function of temperature for yttrium. c) Oxygen and hydrogen depth profiles in yttrium as a function of temperature.

C. *Oxygen sorption in yttrium-based alloys*

Whatever the film composition, a global increase of oxygen content determined by NRA with annealing temperature was observed. For comparison, electrical sheet resistance has been measured and an increase with temperature is also clearly visible [8]. At 300 °C, for yttrium-vanadium and yttrium-titanium based alloys, the sorption of oxygen is related to the amount of yttrium in the film: the quantity of sorbed oxygen atoms is higher in yttrium-rich alloys. As for pure yttrium, the sheet resistance of Y-alloys also increases with the amount of yttrium in the getter, until insulating thin films are obtained. This confirms that electrical measurement provides a good indication of oxygen sorption ability. The ratio between the number of sorbed oxygen and the number of metals for $Y_{64}V_{21}Al_{15}$ is twice larger than for $Y_{20}V_{75}Al_5$. Alloying yttrium with aluminium reduces the oxygen sorption capacity of the film by half.

TEM has been performed on $Y_{32}Ti_{68}$ film annealed at a temperature of 225°C. A gradient of oxygen from the surface to the interface with silicon is clearly visible, the film is not saturated in oxygen. Concerning metal atoms, yttrium content is in-depth homogeneous in the films while titanium appears in the form of grains (Fig. 4).

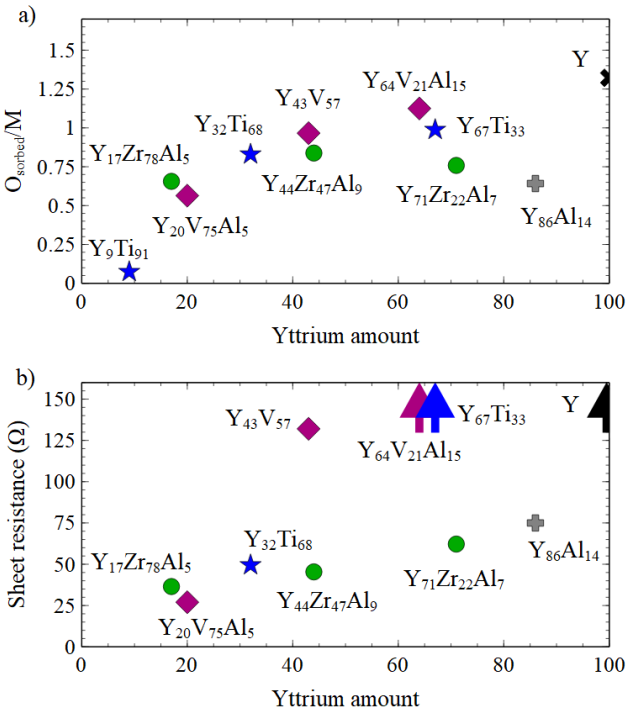

Fig. 3. a) Ratio of sorbed oxygen atoms divided by metal atoms and b) sheet resistance as a function of yttrium amount at 300°C.

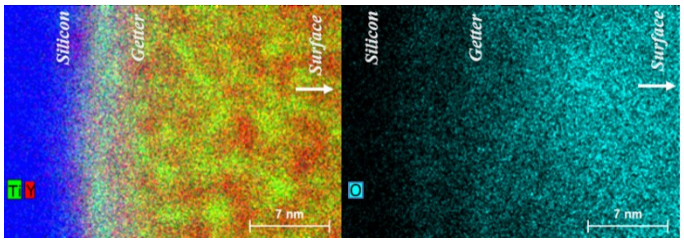

Fig. 4. TEM images of $Y_{32}Ti_{68}$ annealed at 225°C. Left : cartography of yttrium and titanium. Right: cartography of oxygen.

D. *Hydrogen sorption in yttrium-based alloys*

Without annealing treatment, Y-Al, Y-Ti, Y-Zr-Al, Y-V and Y-V-Al alloys exhibit a lower amount of hydrogen than pure yttrium. As shown previously in [8], depth profiles show an hydrogen gradient from the surface to the interface and then a diffusion inside the substrate.

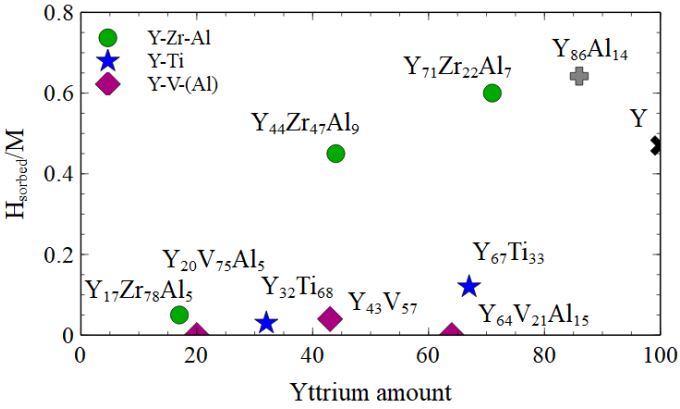

Fig. 5. Ratio of sorbed hydrogen atoms by metal atoms as a function of yttrium amount at 300°C.

After the annealing process, the most efficient alloys for oxygen sorption (i.e Y- Ti and Y-V-Al) show the lowest hydrogen/metal ratio. Getter materials containing aluminium and zirconium exhibit a larger ability to sorb hydrogen as demonstrated in Fig. 5. Fig. 6 shows depth profiles for Y-Al and reveals a very low amount of hydrogen and oxygen for the as-deposited film compared to pure yttrium. However a diffusion of hydrogen in the substrate is also clearly visible. At 300°C, hydrogen is almost homogeneous in-depth while in pure yttrium a concentration gradient was observed.

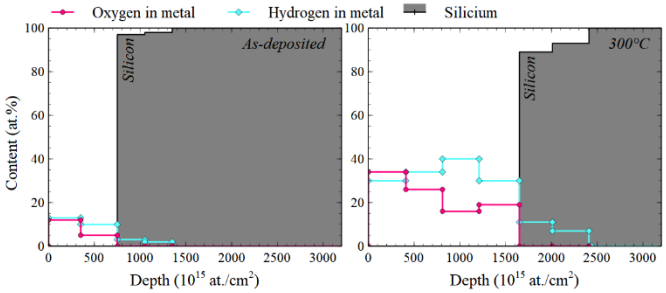

Fig. 6. Oxygen and hydrogen depth profiles in $Y_{86}Al_{14}$ non-annealed and at 300°C.

E. *Summary and conclusion*

Thin films of yttrium-based alloys containing titanium, zirconium, vanadium and/or aluminum were studied by using IBA and electrical characterization to evaluate their ability for oxygen and hydrogen sorption after a thermal treatment. SEM and TEM observations combined with previous XRD analyses were used to characterize their microstructure. The measured in-depth concentration profiles shows that oxygen diffuses into the film from the surface while hydrogen diffuses also in the substrate and is mostly located at the interface with tsilicon. This could be related to the creation of a diffusion barrier for =hydrogen when oxidation becomes high enough. At 300°C, the largest amount of oxygen has been measured for alloys containing vanadium and titanium. The lowest oxygen content was found in alloys containing zirconium and aluminium. Concerning hydrogen sorption, only Y-Zr-Al and Y-Al are highly efficient. Those results show that when thermal activation is not performed in ultra-high vacuum condition, oxidation has a large influence on hydrogen sorption.

As a conclusion, alloys containing yttrium, zirconium and aluminium with a large amount of yttrium seem to be the most promising for both oxygen and hydrogen sorption. Further studies, for example with isotopic gases, will be performed to differentiate diffusion and sorption of species adsorbed on the surface during air exposure and of sorbed gases during annealing.

ACKNOWLEDGMENT

This work was partially funded by the “Agence Nationale de la Recherche” (project ANR-19-CE08-0011), “Nano 2022” program, and by the French RENATECH network. The authors wish to thank Abdelhanin Aassime, Laetitia Leroy, Fabien Bayle, Cédric Villebasse and Ludovic Largeau for their work allowing a good operation of deposition, annealing and characterization set-ups in C2N clean room facilities.

REFERENCES

[1] C. Benvenuti, P. Chiggiato, P. Costa Pinto, A. Escudeiro Santana, T. Hedley, A.Mongelluzzo, V. Ruzinov et I. Wevers, Vacuum properties of TiZrV non-evaporable getter films, Vacuum 60 (2001) 57-65. https://doi.org/10.1016/S0042-207X(00)00246-3.

[2] V. Dragoi, E. Pabo, Wafer bonding technology for new generation vacuum MEMS, Proc. SPIE, 9517, (2015) 951708-1. https://doi.org/10.1117/12.2178920.

[3] A. Bosseboeuf, S. Lemettre, M. Wu, J. Moulin, P. Coste, C. Bessouet, S. Hammami, C. Renard, L. Vincent, Effect of Environment on Activation and Sorption of Getter Alloys and Multilayers for Hybrid Wafer-level Vacuum Packaging, Sens. Mater. 31 (2019) 2825-2849. https://doi.org/10.18494/SAM.2019.2312.

[4] J. N. Huiberts, J. H. Rector, R. J. Wijngaarden, S. Jetten, D. de Groot, B. Dam, N. J. Koeman, R. Griessen, N. Hjörvarsson, S. Olafsson, Y. S. Cho, Synthesis of yttrium trihydride films for ex-situ measurements, J. Alloys Cmpd. 239(1996) 158-171. https://doi.org/10.1016/0925-8388(96)02286-4.

[5] A.E Curzon, O. Singh, Thin film studies of yttrium, yttrium hydrides and yttrium oxide, J. Phys. F: Met. Phys. 8 (1978) 1619-1625. https://doi.org/10.1088/0305-4608/8/8/003.

[6] A. F. Gurbich, SigmaCalc recent development and present status of the evaluated cross-sections for IBA, Nucl. Instr. and Meth. B. 371, (2016) 27-32. https://doi.org/10.1016/j.nimb.2015.09.035.

[7] C. Bessouet, S. Lemettre, C. Kutyla, A. Bosseboeuf, P. Coste, T. Sauvage, H. Lecoq, O. Wendling, A; Bellamy, P. Jagtap, S. Escoubas, C. Guichet, O. Thomas, J. Moulin, Electrical and ion beam analyses of Yttrium and Yttrium-Titanium thin getter films oxidation, J. Vac. Sci. Technol. B 39 (2021) 054202. https://doi.org/10.1116/6.0001084.

[8] C. Kutyla, S. Lemettre, C. Bessouet, A. Bosseboeuf, P. Coste, T. Sauvage, O. Wendling, A, Bellamy, P. Jagtap, S. Escoubas, C. Guichet, O. Thomas, J. Moulin, Hydrogen sorption in yttrium-based getter thin films, Vacuum, EVC-16 Selected Paper, *to be published.*

[9] S. Lemettre et al, “ In-situ electrical characterization of co-evaporated Zr-Ti, Zr-V and Zr-Co thin getter films during thermal activation”, Microsystem Technologies, Volume 25, pp. 4091-4096 (2019)

[10] C. Kittel, “Physique de l’état solide,” Dunod, 8th edition (2007)C. Kittel, “Physique de l’état solide,” Dunod, 8th edition (2007)

[11] V. F. Gantmakher (2011) Mooij rule and weak localization. JETP Lett 94(8):626–628